Are your MRI contrast agents cost-effective?
Learn more about generic Gadolinium-Based Contrast Agents.
FRESENIUS KABI
caring for life

AJNR

This information is current as of April 18, 2024.

Permeability Estimates in Histopathology-Proved Treatment-Induced Necrosis Using Perfusion CT: Can These Add to Other Perfusion Parameters in Differentiating from Recurrent/Progressive Tumors?

R. Jain, J. Narang, L. Schultz, L. Scarpace, S. Saksena, S. Brown, J.P. Rock, M. Rosenblum, J. Gutierrez and T. Mikkelsen

AJNR Am J Neuroradiol 2011, 32 (4) 658-663
doi: https://doi.org/10.3174/ajnr.A2378
http://www.ajnr.org/content/32/4/658

ORIGINAL RESEARCH

Permeability Estimates in Histopathology-Proved Treatment-Induced Necrosis Using Perfusion CT: Can These Add to Other Perfusion Parameters in Differentiating from Recurrent/Progressive Tumors?

R. Jain
J. Narang
L. Schultz
L. Scarpace
S. Saksena
S. Brown
J.P. Rock
M. Rosenblum
J. Gutierrez
T. Mikkelsen

BACKGROUND AND PURPOSE: Differentiating treatment effects from RPT is a common yet challenging task in a busy neuro-oncologic pratice. PS probably represents a different aspect of angiogenesis and vasculature and can provide additional physiologic information about recurrent/progressive enhancing lesions. The purpose of the study was to use PS measured by using PCT to differentiate TIN from RPT in patients with previously irradiated brain tumor who presented with a recurrent/progressive enhancing lesion.

MATERIALS AND METHODS: Seventy-two patients underwent PCT for assessment of a recurrent/progressive enhancing lesion from January 2006 to November 2009. Thirty-eight patients who underwent surgery and histopathologic diagnosis were included in this analysis. Perfusion parameters such as PS, CBV, CBF, and MTT were obtained from the enhancing lesion as well as from the NAWM.

RESULTS: Of 38 patients, 11 were diagnosed with pure TIN and 27 had RPT. Patients with TIN showed significantly lower mean PS values than those with RPT (1.8 ± 0.8 versus 3.6 ± 1.6 mL/100 g/min; *P* value = .001). The TIN group also showed lower rCBV (1.2 ± 0.3 versus 2.1 ± 0.7; *P* value < .001), lower rCBF (1.2 ± 0.5 versus 2.6 ± 1.7; *P* value = .004), and higher rMTT (1.4 ± 0.4 versus 1.0 ± 0.4; *P* value = .018) compared with the RPT group.

CONCLUSIONS: PCT and particularly PS can be used in patients with previously treated brain tumors to differentiate TIN from RPT. PS estimates can help increase the accuracy of PCT in differentiating these 2 entities.

ABBREVIATIONS: BBB = blood-brain barrier; CBF = cerebral blood flow; CBV = cerebral blood volume; EBRT = external beam radiation therapy; FSRT = fractionated stereotactic radiation therapy; GTR = gross total resection; IMRT = intensity-modulated radiation therapy; IV = intravenous; MTT = mean transit time; NAWM = normal-appearing white matter; PCT = perfusion CT; PCV = procarbazine, chloroethyl-cyclohexyl-nitrosourea and vincristine; PS = permeability surface area product; PSR = percentage signal-intensity recovery; rCBF = relative CBF; rCBV = relative CBV; rMTT = relative MTT; ROC = receiver operating characteristic analysis; rPSR = relative PSR; RPT = recurrent/progressive tumor; RT = radiation therapy; SRS = stereotactic radio-surgery; STR = subtotal resection; TIN = treatment-induced necrosis; TMZ = Temozolomide; VEGF = vascular endothelial growth factor; WHO = World Health Organization

Recent advances in brain tumor treatment have led to aggressive management strategies with combinations of surgery, chemotherapy, and radiation therapy based on the location and histologic type of the tumor. Various forms of radiation therapy including SRS, high-dose ERBT, and brachytherapy have become important therapeutic adjuncts. Recent use of cytotoxic and antiangiogenic agents has also increased patient survival and has added to the complexity of imaging responses and recurrence patterns seen in these patients. Differentiating RPT from TIN on imaging studies has always been a challenge. It is imperative to distinguish these conditions as soon as possible to avoid unnecessary antineoplastic treatment if TIN is the predominant pathology and to treat for RPT if that exists. The diagnosis of TIN is best established from tissue obtained at surgical resection. A noninvasive method of diagnosis, however, is desirable to avoid surgery, especially for lesions that are not surgically accessible. Morphologic MR imaging features are usually inadequate to differentiate the 2 entities. In addition, the problem is confounded by the fact that there is often a mixture of tumor with necrosis.

Conventional MR imaging features and MR spectroscopic imaging have been used to differentiate radiation necrosis from recurrent tumors with mixed success.[1-3] Various functional imaging techniques have also been used in the past with limited results.[4] Fluorodeoxyglucose–positron-emission tomography,[5] which is based on tumor glucose metabolism, has shown variable sensitivity and specificity in differentiating recurrent tumors from radiation necrosis and also has limited

Received June 18, 2010; accepted September 10.

From the Division of Neuroradiology, Departments of Radiology (R.J., J.N., S.S.), Neurosurgery (R.J., L. Scarpace, J.P.R., M.R., T.M.), Biostatistics and Research Epidemiology (L. Schultz), Radiation Oncology (S.B.), and Pathology (J.G.), Henry Ford Health System, Detroit, Michigan.

Please address correspondence to Rajan Jain, MD, Division of Neuroradiology, Departments of Radiology and Neurosurgery, Henry Ford Health System, 2799 West Grand Blvd, Detroit MI 48202; e-mail rajanj@rad.hfh.edu

DOI 10.3174/ajnr.A2378

spatial resolution. Posttreatment recurrent enhancing lesions have also been evaluated with MR perfusion imaging, showing increased CBV in recurrent tumors compared with non-neoplastic lesions.[6] PCT has also been used to differentiate recurrent tumors from radiation necrosis on the basis of the difference in blood volume measurements.[7] Most of the perfusion imaging techniques, whether using MR imaging[8,9] or CT, have used only blood volume estimates as a tool to differentiate recurrent high-grade tumor from TIN. However, quantitative estimates of vessel leakiness/permeability, another important physiologic measure of tumor angiogenesis that has been used to grade gliomas preoperatively[10,11] as well as a follow-up tool,[12] have not been used much to differentiate recurrent tumors from TIN.[13,14]

The purpose of this retrospective study was to use quantitative estimates of PS obtained by using PCT in addition to other perfusion parameters in differentiating RPT from TIN in patients with previously irradiated brain tumors.

Materials and Methods

Patient Population

This retrospective study was approved by the institutional review board and was compliant with the Health Insurance Portability and Accountability Act. Between January 2006 and December 2009, 72 patients with recurrent/progressive enhancing lesion noted on the follow-up imaging for a previously treated brain tumor underwent PCT to differentiate RPT from TIN. All these patients had been previously treated with adjuvant radiation and chemotherapy with or without prior surgery. However, only 38 patients who underwent surgery after the PCT examination and histologic confirmation of these recurrent/progressive enhancing lesions were included in the present analysis.

PCT Technique and Parametric Map Analysis

PCT studies were performed on 64-section multidetector row CT scanner (VCT; GE Healthcare, Milwaukee, Wisconsin). A low-radiation-dose noncontrast CT head study was performed to localize the region of interest before obtaining a perfusion scan. For the perfusion scan, 50 mL of nonionic contrast (ioversol, Optiray 350 mg/mL; Mallinckrodt, St. Louis, Missouri) was injected at a rate of 4 mL/s through a 20-ga IV line by using an automatic power injector. At 5 seconds into the injection, a cine (continuous) scan was initiated with the following technique: 80 kVp, 120 mA, and 1 second per rotation for a duration of 50 seconds. After the initial 50-second cine scan, 8 more axial images were acquired, 1 image every 15 seconds for an additional 2 minutes, thus giving a total acquisition time of 199 seconds.[15] The estimated mean effective radiation dose for a PCT study ranges from 3.5 to 3.8 mSv, with the low milliampere protocol used in the present study. Eight 5-mm-thick axial sections were acquired, resulting in a total coverage area of 4 cm. Perfusion maps of CBV, CBF, MTT, and PS were generated at an Advantage Windows workstation by using PCT Advantage Windows 3.0 software (GE Healthcare) in all patients. We used the superior sagittal sinus as the venous output function in all patients and the artery with the greatest peak and slope on time-attenuation curves as the arterial input function. A region of interest was drawn within the confines of a large vessel, and the automatic function of the software picked the pixels with greatest peak and slope on the time-attenuation curve for analysis. Regions of interest were drawn manually on the PCT parametric maps by a neuroradiologist (R.J.), including the whole recurrent enhancing lesion within the coverage region. We placed regions of interest, taking care not to include necrotic/cystic parts or calcified portions of the lesion and also avoiding any major cortical vessels. Another region of interest was also placed over the NAWM in the contralateral cerebral hemisphere. Absolute values of PS for the entire recurrent enhancing lesion, as well as rCBV, rCBF, and rMTT obtained by using the NAWM as the denominator in each case, were used for final analysis.

Histopathologic Examination

TIN was defined as coagulative necrosis accompanied by treatment-related vascular abnormalities, including vessel wall thickening, necrosis, hyalinization, and endothelial proliferation on histopathology. To be eligible for this analysis, the TIN specimen must show no visible tumor (pure TIN) or have only isolated microscopic foci of tumor. Patients in whom TIN tissue was mixed with solid viable tumor were assigned to the RPT group. All cases in which the degree of tumor cell infiltration was questionable were rereviewed by the study neuropathologist (J.G.).

Statistical Analysis

Patient characteristics and treatments for the 2 groups of patients (TIN and RPT) were compared by using χ^2 tests (sex and treatments), 2-sample *t* tests (age), and Wilcoxon 2-sample tests (time from radiation and time between PCT and surgery). Wilcoxon 2-sample tests were performed to compare the PCT parameters between the 2 groups. Multivariate analyses by using logistic regression models were performed to assess the relationship of the PS estimates and other perfusion parameters in differentiating the 2 groups of patients. C-statistics were computed to estimate the area under the curve for these models. In addition, ROCs were performed to determine the best cut-points for the PCT parameters in differentiating TIN and RPT. The cut-points with the highest sum of sensitivity and specificity were selected. All data analyses were conducted by using SAS version 9.2 (SAS Institute, Cary, North Carolina).

Results

Of 38 patients, 11 were diagnosed with pure TIN and 27 had RPT. Thirty-five patients underwent treatment for a primary brain neoplasm (WHO grade II = 7, grade III = 10, grade IV = 18; hemangiopericytoma, $n = 1$), and 3 patients had metastatic disease (brain metastases from lung carcinoma, $n = 2$; skull multiple myeloma, $n = 1$). Thirty-seven patients underwent surgery (STR, $n = 23$; GTR, $n = 9$; biopsy, $n = 5$) for the primary lesion, and 1 patient did not have any surgery. All patients underwent adjuvant radiation therapy (EBRT, 55–60 Gy, $n = 32$; SRS, 14–16 Gy, $n = 3$; IMRT, 5940 cGY, $n = 2$; whole-brain radiation therapy, 54 Gy, $n = 1$) and chemotherapy (in the first cycle of chemotherapy, 28 patients were given TMZ, 3 patients were given bevacizumab, 5 patients received polifeprosan 20 with carmustine implant [Gliadel Wafers], 1 patient received PCV, and 1, carmustine). Four patients received additional SRS ($n = 2$) and a fractionated stereotactic radiation therapy ($n = 2$) boost following the initial EBRT.

The median time interval between development of recurrent/progressive enhancing lesions noted on follow-up imaging and radiation therapy was 15 months (range, 2–150 months). The median time interval between the development of TIN and radiation therapy was 15 months, whereas this time interval was 13 months for the RPT group. Ten patients were on a stable dose of steroids before the PCT examination, whereas 28 patients were not receiving any steroids at the time of

Patient characteristics and treatment information			
	TIN ($n = 11$)	RPT ($n = 27$)	*P* Value
Age (yr), (mean) (range)	45.3 ± 15.1	51.6 ± 13.5	
	(19–73)	(28–79)	.213
Sex (M/F)	9:2	18:9	.350
Extent of first surgery for primary tumor			.762
Biopsy	2 (20%)	3 (11%)	
STR	6 (60%)	17 (63%)	
GTR	2 (20%)	7 (26%)	
Adjuvant therapy			.861
RT + chemotherapy (No.)	10 (91%)	25 (93%)	
RT (No.)	1 (9%)	2 (7%)	
Time interval between RT and appearance of RPT (mo)	15	13	.602
Median (range)	(7–96)	(2–150)	
Steroids at the time of PCT examination (No.)	1 (9%)	9 (33%)	.123
Time between PCT and surgery for the RPT (days)	17	7	.139
(median) (range)	(1–157)	(1–151)	
Extent of second surgery for the RPT			.092
Biopsy (No.)	3 (27%)	1 (4%)	
STR (No.)	7 (64%)	24 (89%)	
GTR (No.)	1 (9%)	2 (7%)	

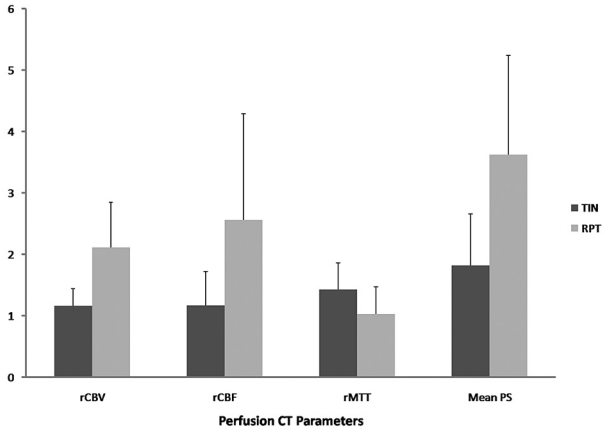

Fig 1. Plot (mean and SD) shows PCT parameters in the TIN and RPT groups.

PCT examination. The median time interval between PCT and surgery for the recurrent/progressive lesion was 11 days (range, 1–157 days). Thirty-four patients underwent surgical resection (STR, $n = 31$; GTR, n = 3), and 4 patients underwent biopsy with multiple specimens obtained for histologic examination (Table). No differences were detected between the 2 groups of patients for patient characteristics and treatments.

PCT Parameters

There was a statistically significant difference between the 2 groups with the TIN group showing significantly lower mean PS values than the RPT group (1.8 ± 0.8 versus 3.6 ± 1.6 mL/100 g/min; *P* value = .001). The TIN group also showed lower rCBV (1.2 ± 0.3 versus 2.1 ± 0.7; *P* value < .001), lower rCBF (1.2 ± 0.5 versus 2.6 ± 1.7; *P* value = .004), and higher rMTT (1.4 ± 0.4 versus 1.0 ± 0.4; *P* value = .018) compared with the RPT group (Figs 1–3). When considered in the same model, both mean PS and rCBV remained significantly associated with differentiating the 2 groups (*P* value = .036 and .031, respectively). The C-statistic for the model with both parameters was 0.956 compared with the 0.877 for mean PS alone and 0.904 for rCBV alone.

From the ROC analyses, high sensitivity and specificity were obtained by using a cutoff value of rCBV > 1.5 (sensitivity, 81.5%; specificity, 90%) and of PS > 2.5 (sensitivity, 81.5%; specificity, 81.8%) to differentiate the 2 entities. Additionally, of the 17 patients with both rCBV > 1.5 and PS > 2.5, all had RPT. In contrast, of the 9 patients with both rCBV ≤ 1.5 and PS ≤ 2.5, eight (89%) had TIN (Fig 4).

Discussion

Radiation-Induced Permeability Changes

Late radiation effects in normal tissues are classically attributed to damage to various critical target-cell populations; in the brain, these 2 cell populations are glial cells and endothelial cells.[16] More recently, the contribution of chronic oxidative stress to late radiation brain injury has been implicated.[17] One school of thought is that endothelial damage is the primary essential event in the pathophysiology of delayed radiation necrosis because the endothelium is relatively vulnerable to reproductive death. The endothelium is sensitive to radiation, but the effect has a longer latency in contrast to the glial cells, which are less sensitive but have a shorter latency. In the first weeks after irradiation, there is a modest but definite breakdown of the BBB; this effect is transitory and is followed by a period of functional recovery and a latent period of normal BBB function.[18,19] However, the endothelial cells have significant irreparable chromosomal damage and reproductive death, leading to a relatively declining number of surviving cells. This latent period, the period of apparent recovery, ends when the number of surviving cells drops below the level required to maintain function, leading to an eventual increase in vascular permeability.[20]

Another study showed that after irradiation, the neuropil seemed morphologically intact at 3.5 months, though necrosis was seen at 4 months after radiosurgery with 75 Gy in the rat cortex.[21] In another rat-model study, it was shown that the BBB breakdown increased up to the 6-month time point and thereafter appeared to stabilize or decrease.[22] Another rat-model study showed detectable disruption of the BBB at 2 weeks postirradiation shown as discrete leakage, whereas late injury seen at 24 weeks indicated more diffuse vascular leakage.[23]

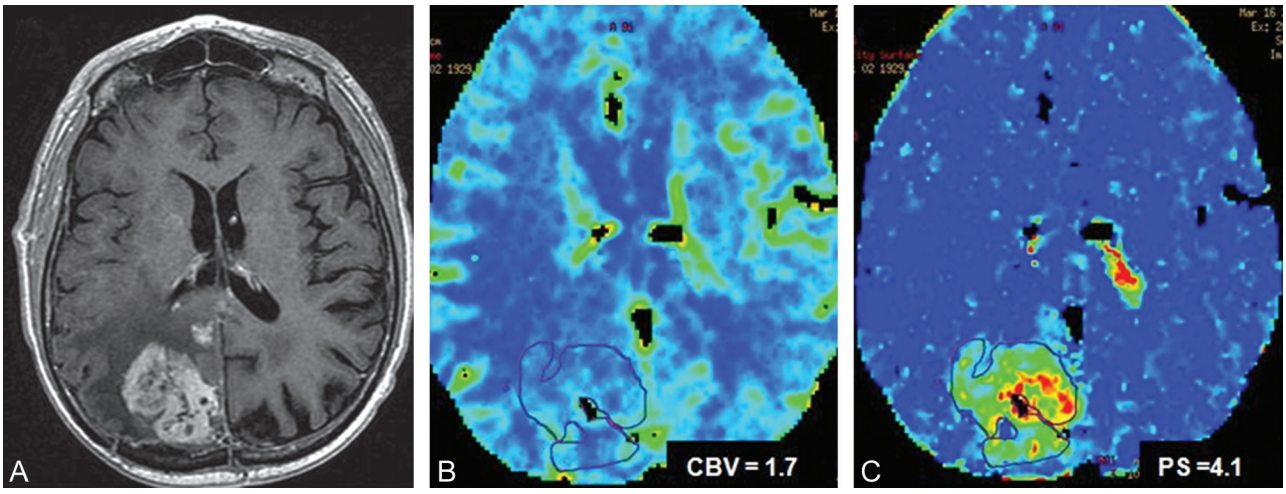

Fig 2. A 77-year-old man with an initial diagnosis of glioblastoma multiforme who underwent GTR, chemotherapy, and RT (EBRT, 60 Gy). *A*, Follow-up MR image shows a recurrent enhancing lesion 26 months post-RT in the right parieto-occipital region within the radiation field. *B* and *C*, CBV (*B*) and PS (*C*) maps show high rCBV and PS, suggesting RPT, which was confirmed with histopathology.

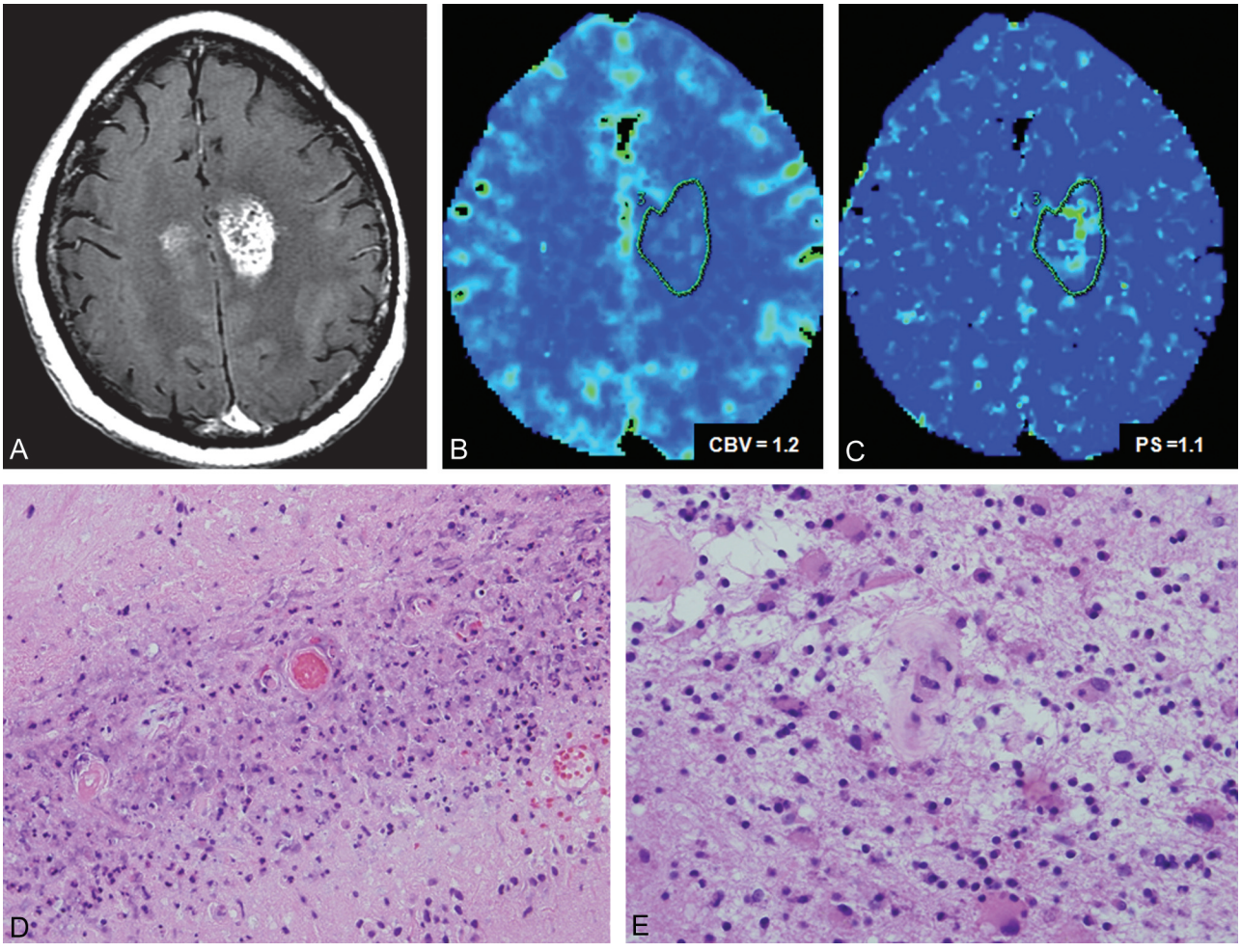

Fig 3. A 41-year-old man with an initial diagnosis of WHO grade II astrocytoma who underwent chemotherapy and RT (IMRT, 63 Gy). *A*, At 33 months post-RT, follow-up MR image shows development of a recurrent enhancing lesion in bilateral frontal regions. *B* and *C*, CBV (*B*) and PS (*C*) maps show low rCBV and PS, suggesting TIN. *D* and *E*, The patient underwent biopsy. Histopathology slides show pan-necrosis, reactive astrocytosis, necrotizing vasculopathy, and demyelination, with no active tumor foci, suggesting TIN (hematoxylin-eosin, original magnification ×10, *D*, and ×20, *E*).

Postradiation therapy permeability changes in the NAWM have also been studied in the past by using dynamic contrast-enhanced MR perfusion techniques.[24,25] Lee et al[25] showed a dose-dependent increase in vascular permeability 2 months after radiation therapy, which decreased at 4 months; however, this study did not have absolute quantification of perme-

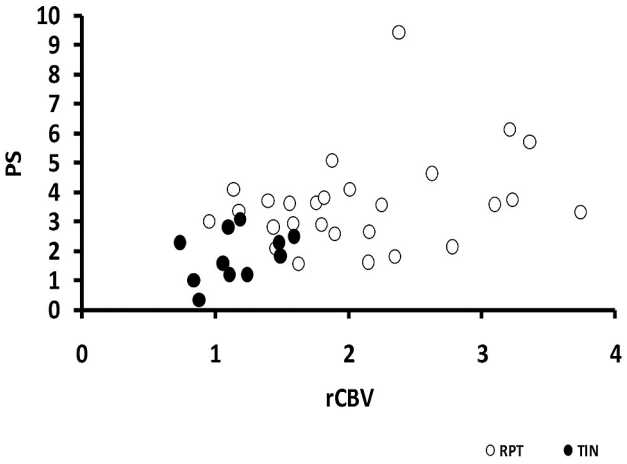

Fig 4. Plot of the association between rCBV and PS for the RPT and TIN groups.

ability, and changes obtained in recirculation phase were presumed to represent vascular permeability. Cao et al[24] also showed an increase in vascular permeability during radiation therapy, which decreased after RT and also was correlated with neurocongnitive dysfunction.

In Vivo Permeability Estimates in Radiation-Induced Injury

Quantitative permeability estimates by using any of the available perfusion imaging techniques have not been performed in the past to differentiate TIN or radiation effects from RPT.[13,14] Part of the reason involves many complexities and assumptions associated with accurate permeability estimates using dynamic contrast-enhanced MR perfusion modalities. Previous authors have used relative PSR or signal-intensity enhancement-time curves as an indirect measure of vascular leakiness successfully; however, absolute quantitative estimates of permeability have not been used yet, to our knowledge, for this very important clinical scenario. Absolute quantitative estimates of PS have been performed by using PCT in brain tumors and have been used for preoperative glioma grading as well as to differentiate high-grade gliomas from non-neoplastic lesions, such as tumefactive demyelinating lesions.[15,26] PS estimates using PCT have shown much more robust results due to a linear relationship of contrast agent with the tissue attenuation curve as well as the availability of a stable arterial input signal intensity compared with MR perfusion techniques. In addition to PS estimates, other hemodynamic perfusion parameters can also be obtained in 1 single experiment by using PCT and, hence, can add to the diagnostic value of the test.

In the present study, we obtained absolute quantification of vascular permeability (ie, PS by using PCT) and have shown increased PS in patients with TIN, but this increased PS is still significantly ($P = .001$) less compared with much more increased PS seen in RPTs. RPTs are usually higher grade tumors with increased vascularity and also increased neoangiogenesis with higher VEGF expression, which leads to increased CBV as well as increased PS, as seen in our observed results. Barajas et al[13] showed lower relative PSR in recurrent glioblastoma multiforme compared with radiation necrosis by using dynamic susceptibility contrast MR perfusion imaging, suggesting a disrupted BBB that was more permeable to macromolecular contrast agents; however, their measurements were not a direct estimate of lesion leakiness. They also noted a large degree of overlap between the 2 groups, making rPSR a less robust predictor of recurrent tumor.[13] The same group also published the same methodology with stronger results by using rPSR to differentiate metastatic tumors from radiation necrosis, suggesting that PSR may be a better prognostic indicator of tumor recurrence than rCBV,[27] hence probably, to some degree, exposing the limitations of nonquantitative and indirect methods of permeability assessment.

Practical Problems Using Permeability Estimates to Differentiate TIN From RPT

Apart from the limited resolution of clinically available imaging tools for permeability estimates in RPTs, most of these lesions have viable tumor mixed with variable amounts of tumor or treatment-induced necrosis. This combination not only leads to a very heterogeneous morphologic imaging appearance but also restricts the utility of most of the functional imaging modalities. Most of these modalities, whether using metabolic or physiologic imaging, are banking on the differences in metabolic or physiologic demands of the tissue. Another factor that can particularly complicate permeability estimates is the fact that upregulation of VEGF, which is known to be 1 of the major factors responsible for increased leakiness of blood vessels in tumors,[28] and is also upregulated in radiation injury.[29] Recent reports suggesting that anti-VEGF therapy can be used in patients with radiation necrosis supports the role played by VEGF signaling cascade in radiation injury.[30,31]

Vascular Perfusion Parameters in Differentiating TIN from RPT

Blood volume estimates obtained by using MR[8,11,27] or PCT[7] techniques have been previously used with significant success in differentiating the 2 entities. Blood volume estimates are based on the differences in vascularity of the 2 entities, with recurrent tumors showing high blood volume due to tumor angiogenesis and increased vascular density; whereas radiation necrosis shows low blood volume because it consists primarily of hyalinized vasculopathy and coagulative necrosis, leading to hypoperfusion. However, tumor vasculature and perfusion also depend on a number of other variables and are usually very heterogeneous. In a rapidly growing high-grade tumor, vasculature can be severely compromised due to the rapid growth of the tumor cells, necrosis, and increased permeability of the vessels causing interstitial edema, which can result in compression of the smaller vessels, also leading to areas of hypoperfusion. Similarly, within irradiated brain tissue, in addition to occlusive vasculopathy, a variety of other vascular phenomena are noted, such as aneurysmal formation, telangiectasia, vascular elongation, and a remarkable proliferation of endothelial cells, especially in the capillary bed,[32] which can even increase CBV in radiation necrosis, thus inducing some overlap of the vascular perfusion parameters. Hence, the addition of permeability measurements, as in the present study, can provide another aspect of the vasculature that may help differentiate the 2 entities better.

CBV and PS, even though they are probably correlated, have been shown to represent different aspects of tumor angiogenesis in a recent publication.[28] CBV has been shown to

correlate with microvascular density, whereas PS has shown a stronger correlation with microvascular cellular proliferation.[28] In the present study, we showed a similar association of rCBV and PS (Fig 4), with some patients showing lower rCBV but high PS and vice versa, suggesting that the perfusion imaging modalities that will provide estimates of both CBV and PS may help better differentiate non-neoplastic lesions such as TIN from RPT. However, most of the commercially available perfusion software is vendor-specific and uses different postprocessing methodology; hence, absolute or even relative values of perfusion parameters obtained by using one software may not match those in another center using a different vendor and software. However, understanding the histologic and angiogenic bases of these perfusion parameters will help in better use of these imaging tools, especially in clinical practice, where most of these recurrent enhancing lesions consist of variable degrees of viable tumor and necrosis.

Limitations of the Study

One of the major limitations of our study is the small sample size, particularly of histopathology-proved radiation necrosis, apart from being a retrospective study. Another important factor is that 9 (33%) patients with RPT were on stable doses of steroids at the time of PCT examination compared with only 1 (9%) of the patients with TIN, which could potentially lead to erroneous estimates of permeability because steroids are known to repair the damaged BBB. However, if that is the case, in fact, this will enhance our statistically significant results by increasing PS estimates further in the RPT group. Another limitation of our study is that 3 (27%) of the patients with TIN were diagnosed with biopsies, which may not be a true representative of the whole lesion; however, 2 of these 3 patients had stable or improving enhancing lesion on follow-up MR imaging studies.

Conclusions

Permeability estimates can provide additional physiologic information about recurrent/progressive enhancing lesions in addition to the other vascular parameters by using PCT, which can aid in differentiating TIN from RPT. Radiation necrosis shows lower PS compared with RPT due to leaky angiogenesis seen with high-grade recurrent tumors, whereas vasculature associated with TIN is not that leaky, despite having damaged endothelium and hypoxia-related VEGF upregulation.

References

1. Cheronov M, Hayashi M, Izawa M, et al. **Differentiation of the radiation-induced necrosis and tumor recurrence after gamma knife radiosurgery for brain metastases: importance of multivoxel proton MRS.** *Minim Invasive Neurosurg* 2005;48:228–34
2. Graves EE, Nelson SJ, Vigneron DB, et al. **Serial proton MR spectroscopic imaging of recurrent malignant gliomas after gamma knife radiosurgery.** *AJNR Am J Neuroradiol* 2001;22:613–24
3. Kumar AJ, Leeds NE, Fuller GN, et al. **Malignant gliomas: MR imaging spectrum of radiation therapy- and chemotherapy-induced necrosis of the brain after treatment.** *Radiology* 2000;217:377–84
4. Jain R, Narang J, Sundgren PM, et al. **Treatment induced necrosis versus recurrent/progressing brain tumor: going beyond the boundaries of conventional morphologic imaging**. *J Neurooncol* 2010;100:17–29. Epub 2010 Feb 24
5. Langleben DD, Segall GM. **PET in differentiation of recurrent brain tumor from radiation injury.** *J Nucl Med* 2000;41:1861–67
6. Covarrubias DJ, Rosen BR, Lev H. **Dynamic magnetic resonance perfusion imaging of brain tumors.** *Oncologist* 2004;9:528–37
7. Jain R, Scarpace L, Ellika S, et al. **First-pass perfusion computed tomography: initial experience in differentiating recurrent brain tumors from radiation effects and radiation necrosis.** *Neurosurgery* 2007;61:778–86
8. Cha S, Lupo JM, Chen MH, et al. **Differentiation of glioblastoma multiforme and single brain metastasis by peak height and percentage of signal intensity recovery derived from dynamic susceptibility-weighted contrast-enhanced perfusion MR imaging.** *AJNR Am J Neuroradiol* 2007;28:1078–84
9. Hu LS, Baxter LC, Smith KA, et al. **Relative cerebral blood volume values to differentiate high-grade glioma recurrence from post treatment radiation effect: direct correlation between image-guided tissue histopathology and localized dynamic susceptibility-weighted contrast-enhanced perfusion MR imaging measurements.** *AJNR Am J Neuroradiol* 2009;30:552–58
10. Ellika SK, Jain R, Patel SC, et al. **Role of perfusion CT in glioma grading and comparison with conventional MR imaging features.** *AJNR Am J Neuroradiol* 2007;28:1981–87
11. Law M, Yang S, Babb JS, et al. **Comparison of cerebral blood volume and vascular permeability from dynamic susceptibility contrast-enhanced perfusion MR imaging with glioma grade.** *AJNR Am J Neuroradiol* 2004;25:746–55
12. Sorensen AG, Batchelor TT, Zhang WT, et al. **A "vascular normalization index" as potential mechanistic biomarker to predict survival after a single dose of cediranib in recurrent glioblastoma patients.** *Cancer Res* 2009;69:5296–300. Epub 2009 Jun 23
13. Barajas RF Jr, Chang JS, Segal MR, et al. **Differentiation of recurrent glioblastoma multiforme from radiation necrosis after external beam radiation therapy with dynamic susceptibility-weighted contrast-enhanced perfusion MR imaging.** *Radiology* 2009;253:486–96
14. Hazle JD, Jackson EF, Schomer DF, et al. **Dynamic imaging of intracranial lesions using fast spin-echo imaging: differentiation of brain tumors and treatment effects.** *J Magn Reson Imaging* 1997;7:1084–93
15. Jain R, Ellika SK, Scarpace L, et al. **Quantitative estimation of permeability surface-area product in astroglial brain tumors using perfusion CT and correlation with histopathologic grade.** *AJNR Am J Neuroradiol* 2008;29:694–700
16. Hopewell JW, Wright EA. **The nature of latent cerebral irradiation damage and its modification by hypertension.** *Br J Radiol* 1970;43:161–67
17. Zhao W, Diz DI, Robbins ME. **Oxidative damage pathways in relation to normal tissue injury.** *Br J Radiol* 2007;80:S23–31
18. Lundqvist H, Rosander K, Lomanov M, et al. **Permeability of the blood-brain barrier in the rat after local proton irradiation.** *Acta Radiol Oncol* 1982;21:267–71
19. Remler MP, Marcussen WH. **Time course of early delayed blood-brain barrier changes in individual cats after ionizing radiation.** *Exp Neurol* 1981;73:310–14
20. Remler MP, Marcussen WH, Tiller-Borsich J. **The late effects of radiation on the blood brain barrier.** *Int J Radiat Oncol Biol Phys* 1986;12:1965–69
21. Kamiryo T, Lopes MB, Kassell NF, et al. **Radiosurgery-induced microvascular alterations precede necrosis of the brain neuropil.** *Neurosurgery* 2001;49:409–14, discussion 414–15
22. Bernstein M, Marotta T, Stewart P, et al. **Brain damage from 125I brachytherapy evaluated by MR imaging, a blood-brain barrier tracer, and light and electron microscopy in a rat model.** *J Neurosurg* 1990;73:585–93
23. Rubin P, Gash DM, Hansen JT, et al. **Disruption of the blood-brain barrier as the primary effect of CNS irradiation.** *Radiother Oncol* 1994;31:51–60
24. Cao Y, Tsien CI, Sundgren PC, et al. **Dynamic contrast-enhanced magnetic resonance imaging as a biomarker for prediction of radiation-induced neurocognitive dysfunction.** *Clin Cancer Res* 2009;15:1747–54
25. Lee MC, Cha S, Chang SM, et al. **Dynamic susceptibility contrast perfusion imaging of radiation effects in normal-appearing brain tissue: changes in the first-pass and recirculation phases.** *J Magn Reson Imaging* 2005;21:683–93
26. Jain R, Ellika S, Lehman NL, et al. **Can permeability measurements add to blood volume measurements in differentiating tumefactive demyelinating lesions from high grade gliomas using perfusion CT?** *J Neurooncol* 2010;97:383–88
27. Barajas RF, Chang JS, Sneed PK, et al. **Distinguishing recurrent intra-axial metastatic tumor from radiation necrosis following gamma knife radiosurgery using dynamic susceptibility-weighted contrast-enhanced perfusion MR imaging.** *AJNR Am J Neuroradiol* 2009;30:367–72
28. Jain R, Gutierrez J, Narang J, et al. **In vivo correlation of tumor blood volume and permeability with histological and molecular angiogenic markers in gliomas**. *AJNR Am J Neuroradiol* 2011;32:388–94
29. Nordal RA, Nagy A, Pintilie M, et al. **Hypoxia and hypoxia-inducible factor-1 target genes in central nervous system radiation injury: a role for vascular endothelial growth factor.** *Clin Cancer Res* 2004;10:3342–53
30. Gonzalez J, Kumar AJ, Conrad CA, et al. **Effect of bevacizumab on radiation necrosis of the brain.** *Int J Radiat Oncol Biol Phys* 2007;67:323–26
31. Torcuator R, Zuniga R, Mohan YS, et al. **Initial experience with bevacizumab treatment for biopsy confirmed cerebral radiation necrosis.** *J Neurooncol* 2009;94:63–68
32. Gaensler EH, Dillon WP, Edwards MS, et al. **Radiation-induced telangiectasia in the brain simulates cryptic vascular malformations at MR imaging.** *Radiology* 1994;193:629–36